Supporting Information

Thermal evaporation-driven fabrication of Ru/RuO_2 nanoparticles onto nickel foam for efficient overall water splitting

Yan Hou[a], Zheng Qin[a], Xu Han[a], Yingxin Liu[a], Wei Zhang[a], Xueqin Cao[a], Yongyong Cao[*b], Jian-Ping Lang[*a] and Hongwei Gu[*a]

Table of Contents

1.Experimental section

Materials and reagents

Acetone, ethanol and isopropanol were purchased from Sinopharm Group Chemical Reagent Co., Ltd. Nafion solution (0.5 wt %), commercial 20 wt% Pt/C were purchased from Sigma-Aldrich. Commercial RuO_2 was purchased from Shanghai yuanye Bio-Technology Co., Ltd. Hydrochloric acid (HCl) was purchased from Chinasun Specialty Products Co., Ltd. Ltd. Triruthenium dodecacarbonyl ($Ru_3(CO)_{12}$, marked as Ru_1) was purchased from Adamas Reagent Co., Ltd. Ruthenium acetylacetonate ($Ru(acac)_3$) was purchased from Shanghai Haohong Scientific Co., Ltd. Ni foam (NF, thicknesses: 1 mm) was purchased from Taiyuan Lizhiyuan Technology Co., Ltd. All the chemicals were analytical purity and used as received without any further purification unless stated otherwise.

Material characterization

The morphologys of samples were characterized by scanning electron microscope (SEM, Hitachi S-4700), transmission electron microscope (TEM, TecnaiG220, FEI). The X-ray diffraction (XRD) patterns of synthesized catalysts were tested by X'Pert-Pro MPD diffractometer (Netherlands PANalytical) with a Cu Kα X-ray source (λ = 1.540598 Å). Elemental analysis of C, Ru, Ni and O in the samples was detected by SEM-energy-dispersive-X-ray spectroscopy (SEM-EDX). The larger-magnified nanostructure and EDX elemental mapping were characterized using a high-resolution TEM (HRTEM, Talos F200X G2). To further analyze the surface electronic structure of the nanomaterials, X-ray photoelectron spectroscopy (XPS, Escalab250Xi, UK) was performed using a hemispherical electron energy analyzer.

Preparation of commercial comparison electrodes

20 wt% Pt/C and RuO_2 electrodes:

5 mg of 20 wt% Pt/C was added into a mixed solution consisting of isopropanol (970 μL) and Nafion solution (30 μL). After ultrasonic treatment for at least 30 min, 30 μL of the as-obtained homogeneous ink solution was dropped onto a bare nickle foam (0.5 cm × 0.5 cm). And the commercial RuO_2 electrode was made via a similar process.

Calculation of Ru mass loading in Ru/NF

Firstly, the 20 pieces of the Ru/NF with the same diameter of 2 cm were immersed into concentrated HCl under vigorously stirring. The acid-soluble Ni was removed by HCl after stirring for 3 days at room temperature and a black powder of Ru was carefully centrifuged off, washed and dried at 100 °C for 24 h

under vacuum condition. Then, the mass loading of Ru in the Ru/NF was calculated to be ~0.15 mg cm^{-2}.

Electrochemical measurements

Electrochemical measurements were conducted on a CHI760E electrochemical workstation at room temperature by using a three-electrode cell, typically with a reference electrode (saturated Ag/AgCl), a counter electrode (graphite rod), and a working electrode (Ru/NF). To prepare the sample electrode, the Ru/NF (2.0 cm × 2.0 cm) was cut into 0.5 cm × 1.0 cm for subsequent electrochemical test, and the actual effective area contacting with the electrolyte is 0.25 cm^2. The electrodes of other samples (Ru_1 /NF, Ru_2/NF, etc.) for HER and OER were prepared via the same way. All the presented potentials were 95% iR corrected unless otherwise indicated, followed by conversion to the RHE scale using the Nernst equation: ERHE= Esaturated Ag/AgCl+ 0.0591 × pH+ 0.197. LSV polarization curves for HER and OER were recorded at a scan rate of 5 mVs^{-1}. The overpotential (η) values of OER were calculated according to formula: η = ERHE − 1.23 V. The HER and OER durability of the catalyst were checked through chronopotentiometry at a current density of 10 mA cm^{-2} in 1.0 M KOH. In a non-faradaic region, the electrochemical double layer capacitance (C_{dl}) can be calculated from the cyclic voltammograms measured at different scan rates (v = 20, 40, 60, 80 and 100 mV s^{-1}). The current density difference of the half-potential at the same sweep speed against the scan rates were plotted and fitted to obtain C_{dl} values. Electrochemical impedance spectroscopy (EIS) was measured in the frequency scan range from 0.01 kHz to 100 kHz.

Density functional theory computations

We performed density functional theory (DFT) computations based on first principles via the Vienna ab initio simulationpackage (VASP). The generalized gradient approximation (GGA) with the Perdew–Burke–Ernzerhof (PBE) exchange–correlation functional was chosen to describe the exchange–correlation interactions and the DFT-D3 method waschosen tocorrectly describe van der Waals (vdW) interactions [1,2]. The projected augmented wave (PAW) was used todescribe the interaction between the nucleus and the valence electrons [3]. The cutoff energy of the plane-wave basis set was set as 520.00 eV, and the convergence criteria for energy andforce on each atom during geometry optimization were set to10^{-5} eV and 0.05 eV/Å, respectively. The 4 × 4 × 1 Monkhorst–Pack grid k-points were adopted to optimized the structures of Ru, RuO_2 and Ru/RuO_2. The vacuum layer was set to 15.00 Å to avoid interaction between the periodic structures. Bader charge analysis was adapted to calculate the charge transfer between the substrate and adsorbates [4,5]. The Gibbs free energy profile diagram was calculated using the computational hydrogen electrode model (CHE) proposed by Nørskov et al [6].

The Gibbs free energy of each elementary step was obtained through the following equation:

$\Delta G = \Delta E + \Delta EZPE + \int Cp\, dT - T\Delta S$

where ΔE is the free energy change that can be obtained from DFT calculations, ΔEZPE is the zero-point energy correction, and T and ΔS are the temperature and entropy, respectively. ∫Cp dT is the enthalpic temperature correction, and considering at a temperature of 298.15 K.

The overpotential (η) values of the OER can be obtained by:

$\eta = \max [\Delta G_1, \Delta G_2, \Delta G_3, \Delta G_4]/e - 1.23$

where the ΔG_1, ΔG_2, ΔG_3, ΔG_4 are the free energy for four elementary reactions of OER.

2. Supplementary figures

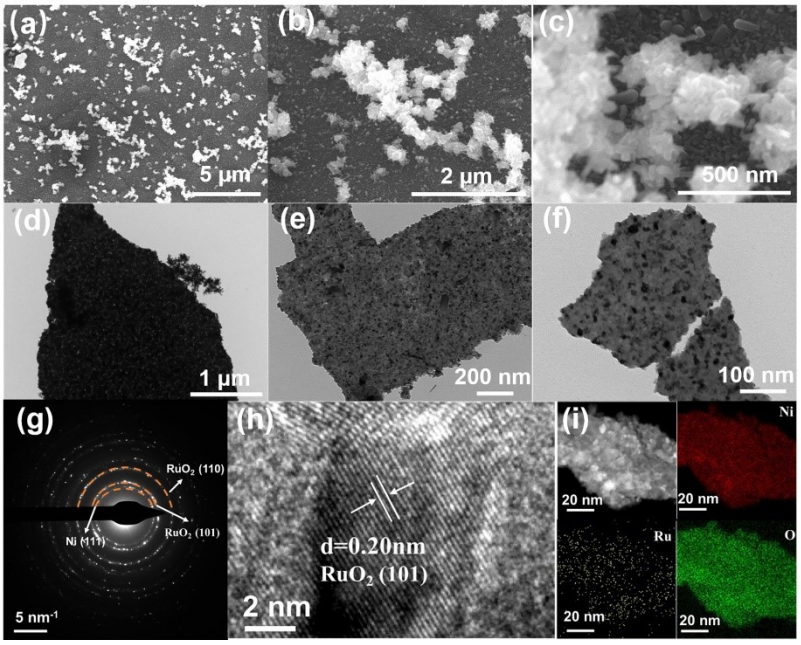

Fig. S1 (a-c) SEM images of Ru_1/NF. (d-f) TEM images of Ru_1/NF. (g) SAED pattern of Ru_1/NF. (h) The HRTEM image of Ru_1/NF. (i) HAADF-STEM image and elemental mapping of Ni, Ru, O in the image of Ru_1/NF.

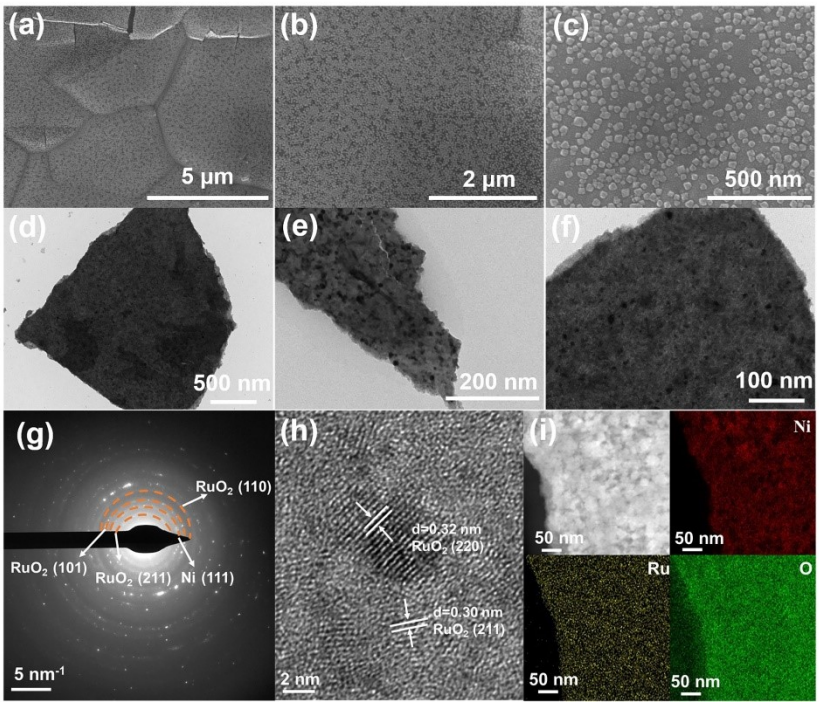

Fig. S2(a-c) SEM images of Ru_2/NF. (d-f) TEM images of Ru_2/NF. (g) SAED pattern of Ru_2/NF. (h) The HRTEM image of Ru_2/NF. (i) HAADF-STEM image and elemental mapping of Ni, Ru, O in the image of Ru_2/NF.

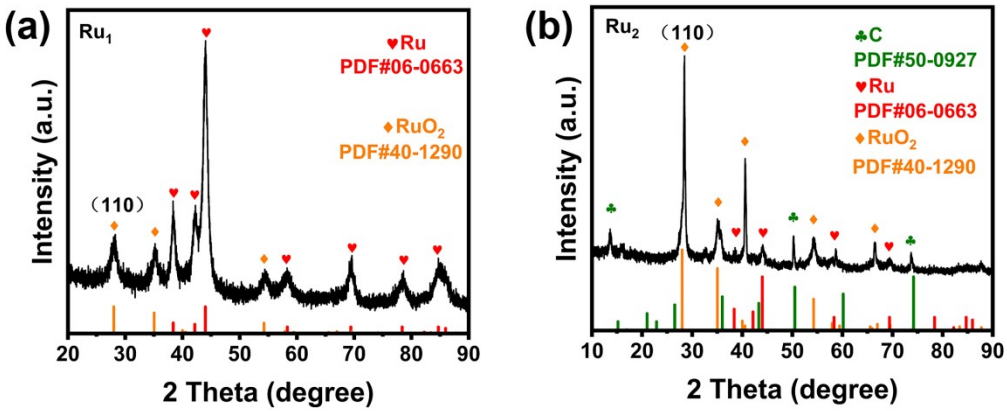

Fig. S3 PXRD patterns of the Ru_1 and the Ru_2.

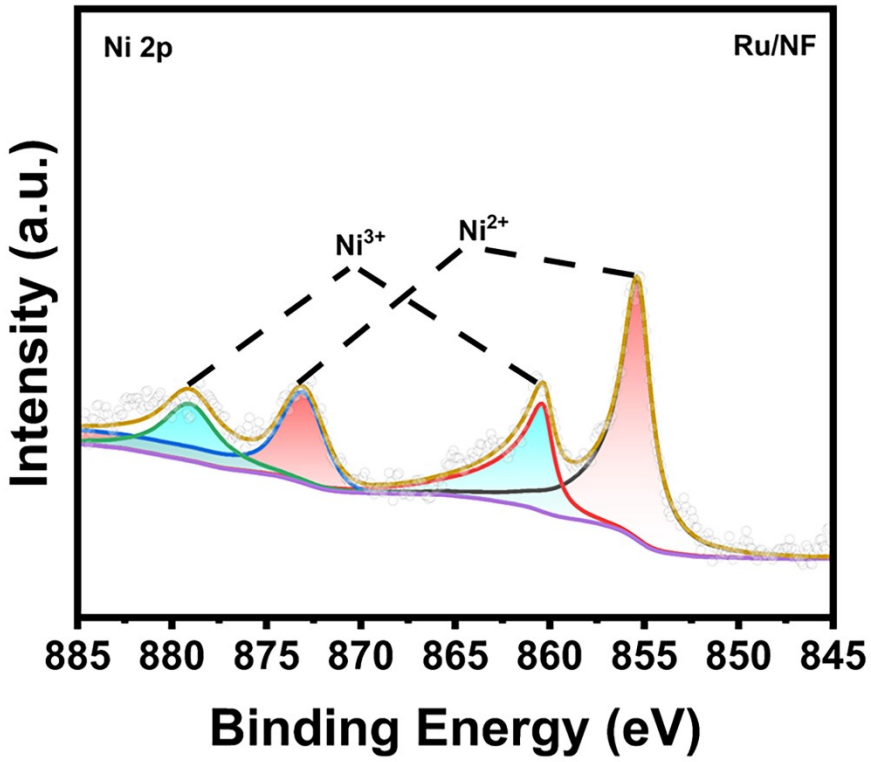

Fig. S4 High-resolution XPS spectrum for Ni 2p after CP test at anode current.

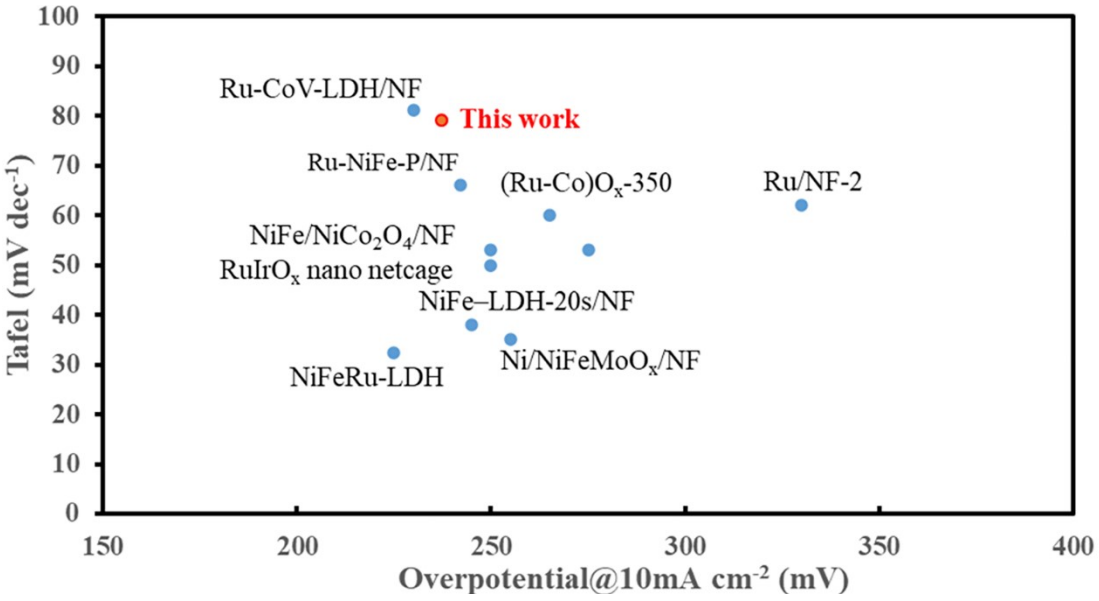

Fig. S5 Comparison of recent OER electrocatalysts in alkaline electrolytes.

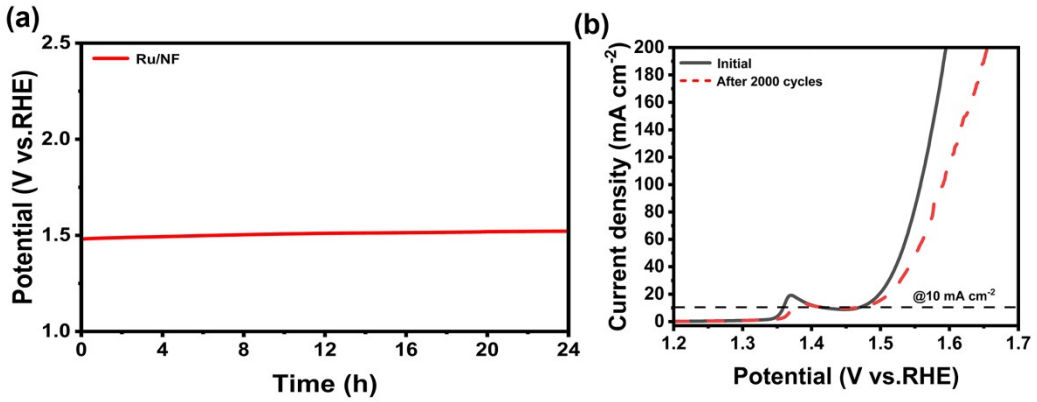

Fig. S6 (a) The chronopotentiometry test of Ru/NF. (b) LSV curves of Ru/NF before and after 2000 CV cycles.

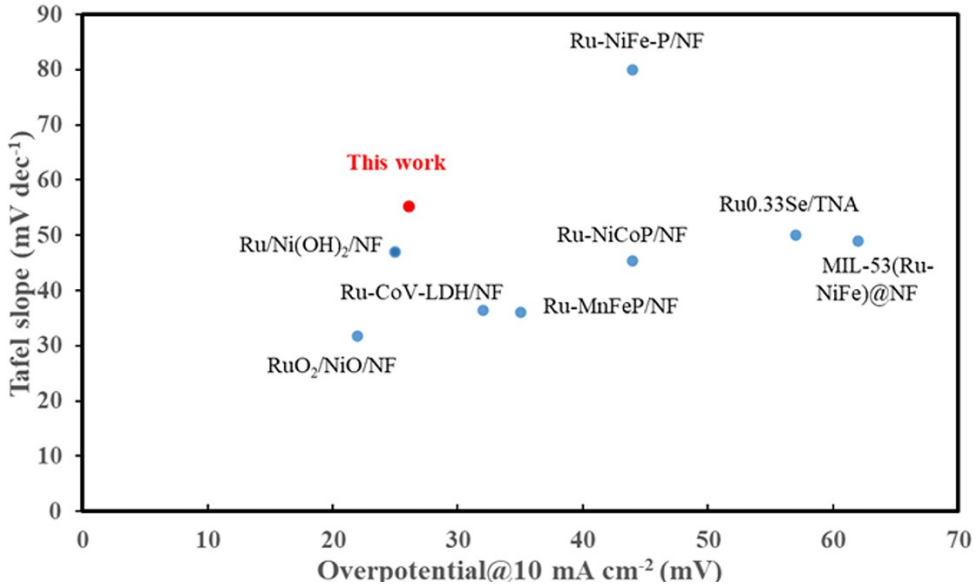

Fig.S7 Comparison of recent HER electrocatalysts in alkaline electrolytes

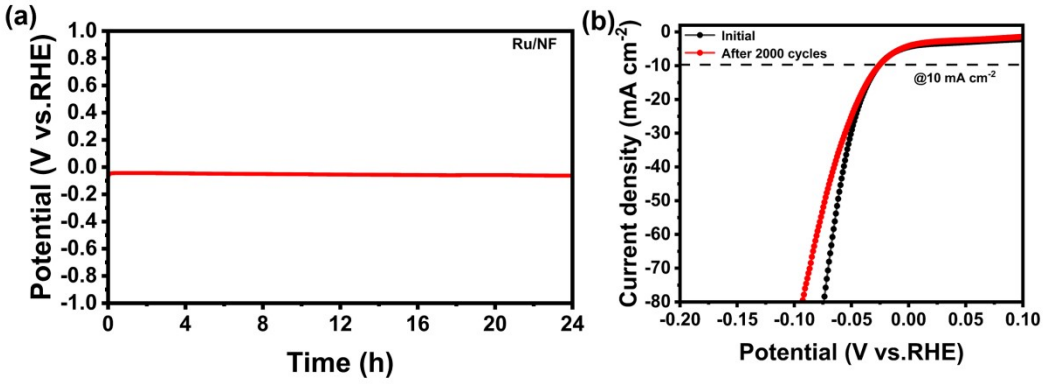

Fig. S8 (a) The chronopotentiometry test of Ru/NF. (b) LSV curves of Ru/NF before and after 2000 CV cycles.

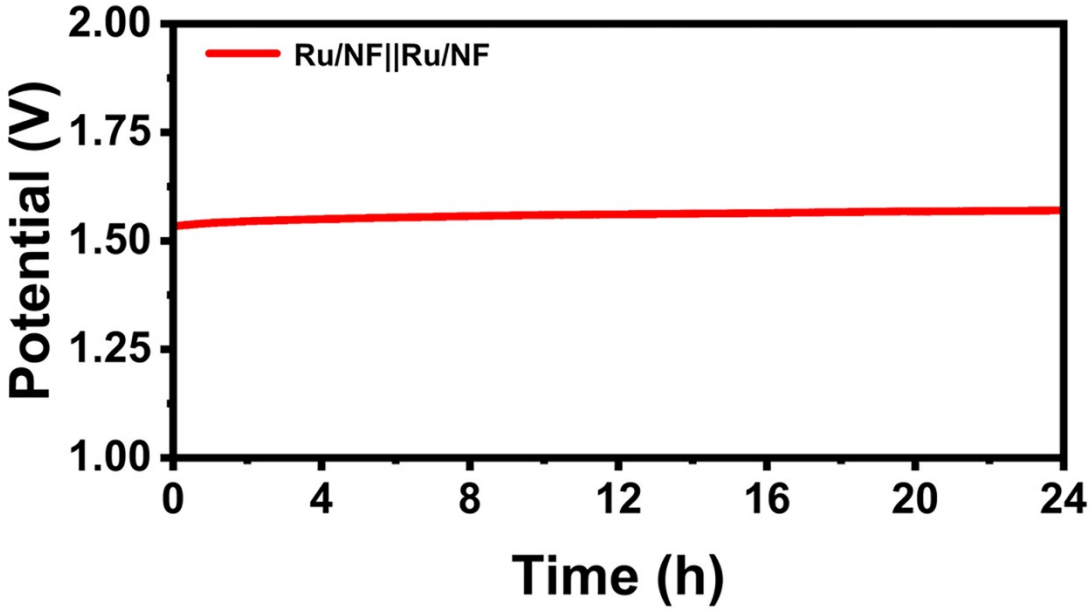

Fig. S9 The chronopotentiometry test of Ru/NF||Ru/NF.

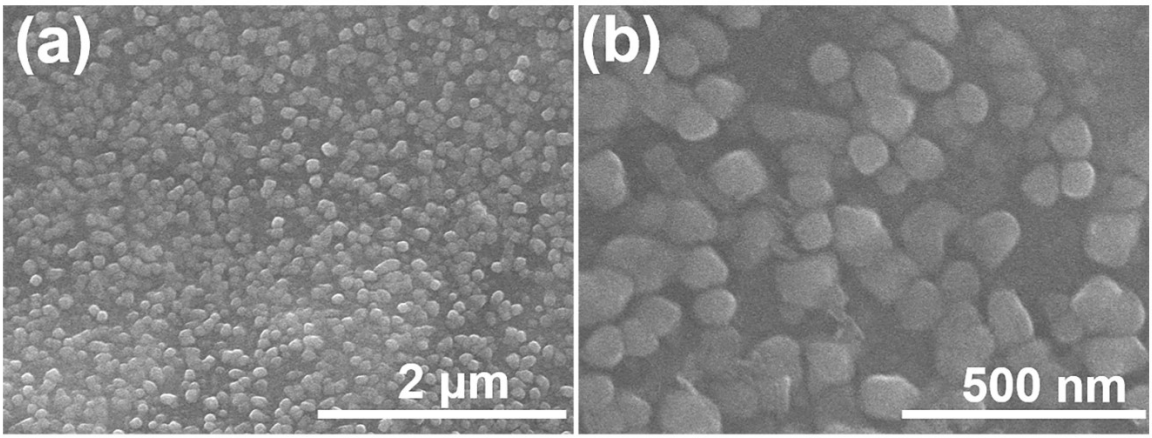

Fig. S10 SEM images of (a-b) Ru/NF after CP test during overall water splitting.

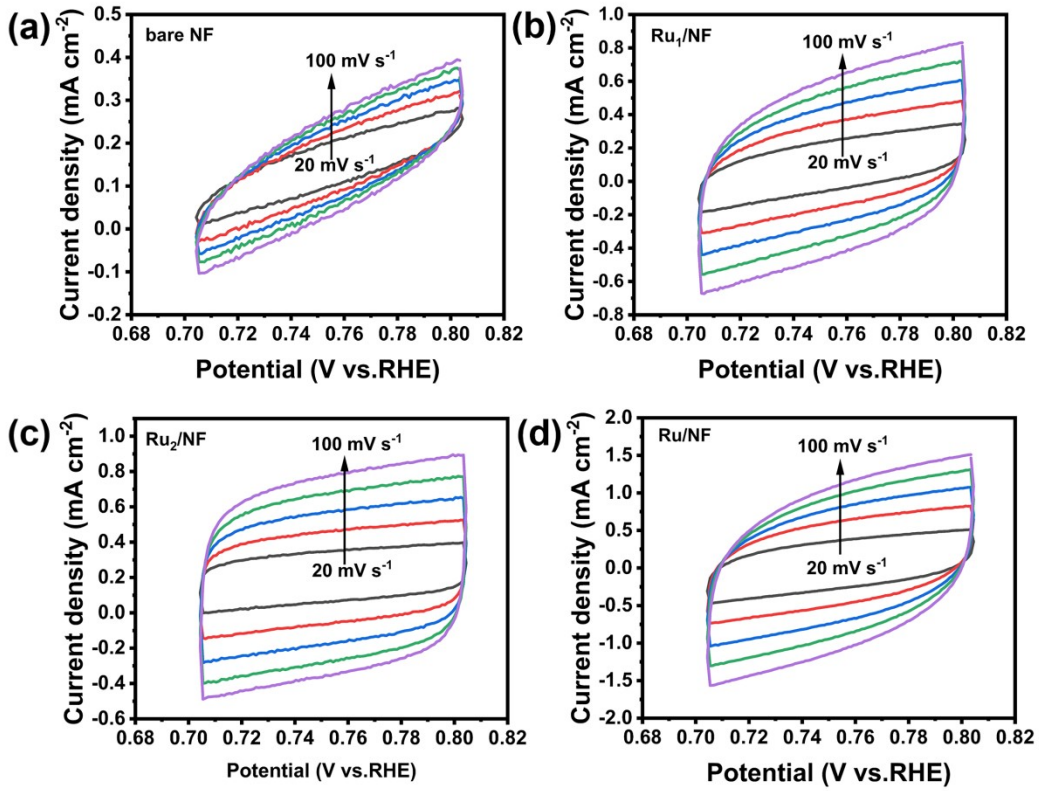

Fig. S11 CV curves of (a) bare NF, (b) Ru_1/NF, (c) Ru_2/NF and (d) Ru/NF with different scan rates from 20 to 100 mV s^{-1}.

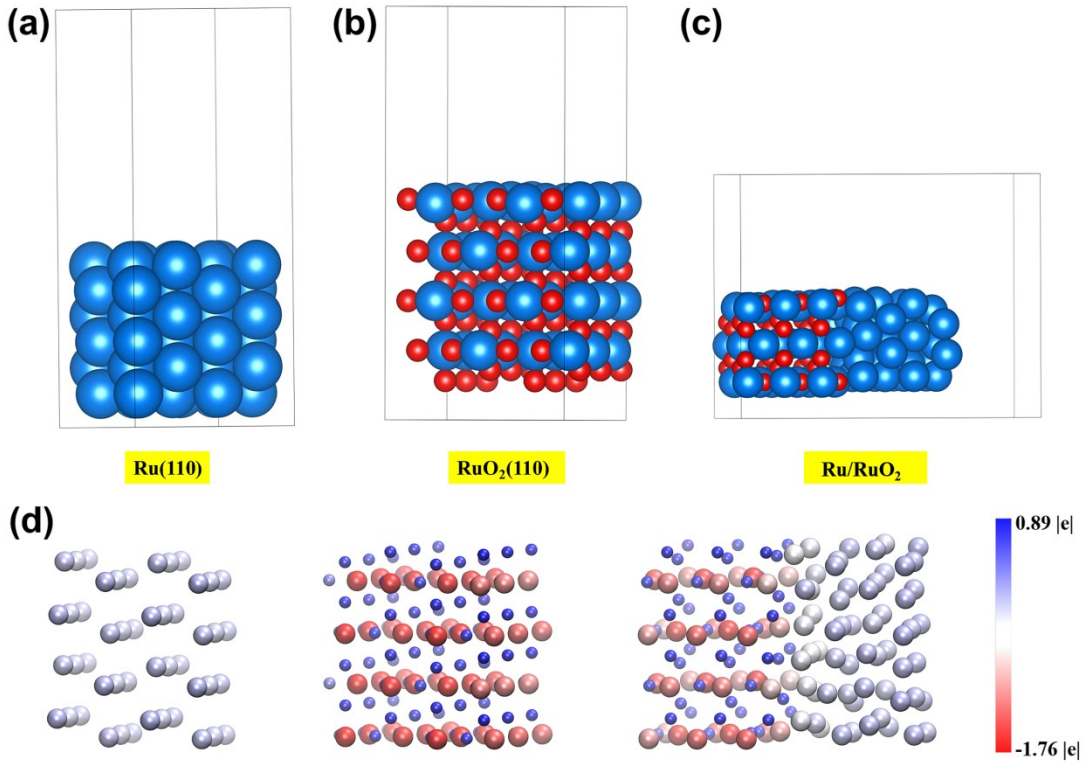

Fig. S12 (a-c) The computational models of Ru, RuO_2 and Ru@RuO_2. (d) Bader charge analysis.

3 Supplementary table

Table S1. Comparison of recent bifunctional electrocatalysts supported on NF for overall water splitting in alkaline electrolytes.

Catalysts	Electrolyte	HER η_{10}（mV）	HER Tafel slope (mV dec^{-1})	OER η_{10}（mV）	OER Tafel slope (mV dec^{-1})	E_{10} (V)	Ref.
Ru/NF	1 M KOH	26.1	55.21	235.4	78.98	1.50	This work
Ru-FeRu@C/NC	1 M KOH	23	23.7	345	64.7	1.63	7
Ru-G/CC||Ru-H_2O/CC-350	1 M KOH	40	76	270	63	1.67	8
Fe-Co-O/Co@NC-mNS/NF	1 M KOH	112	96	257	41.56	1.58	9
NiFe-LDH@CoSx/NF	1 M KOH	136	73	206	62	1.537	10
Ru-NiCoP/NF	1 M KOH	44	45.4	216	84.5	1.515	11
Ru-MnFeP/NF	1 M KOH	35	36	191$^{\#}$	69$^{\#}$	1.47	12
CoRu-MoS_2	1 M KOH	52	55	308	50	1.67$^{\#}$	13
NF/T(Ni_3S_2/MnS-O)	1 M KOH	116	41	228	46	1.54	14
NiVRu-LDH||NiVIr-LDH	1 M KOH	12	40	180	38	1.42	15
RuO_2/NiO/NF	1 M KOH	22	31.7	250	50.5	1.5	16
NiFe LDH@NiCoP/NF	1 M KOH	120	88.2	220	48.6	1.57	17

Noted: Value marked with a "*" means that water splitting appears in an asymmetric electrolyzer. Value marked with a "#" means that overpotential at 20 mA cm^{-2}.

References

1 J. Perdew, J. Chevary, S. Vosko, K. Jackson, M. Pederson, D. Singh andC. Fiolhais, *Phys. Rev. B.*, 1992, **46***,* 6671-6687.

2 P. John, B. Kieron and E. Matthias, *Phys. Rev. Lett*., 1996, **77**, 3865.

3 P. Blöchl, *Phys. Rev. B*., 1994, **50**, 17953-17979.

4 G. Henkelman, A. Arnaldsson and H. Jónsson. *Comp. Mater. Sci*., 2006, **36**, 354- 360.

5 E. Sanville, S. Kenny, R. Smith and G. Henkelman., *J. Comput. Chem*. 2007, **28**, 899-908.

6 A. Peterson, F. Abild-Pedersen, F. Studt, J. Rossmeisl and J. Nørskov, *Energy Environ. Sci.*, 2010, **3**, 1311-1315.

7 W. Feng, Y. Feng, J. Chen, H. Wang, Y. Hu, T. Luo, C. Yuan, L. Cao, L. Feng and J. Huang, *Chem. Eng. J*., 2022, **437**, 135456.

8 M. You, X. Du, X. Hou, Z. Wang, Y. Zhou, H. Ji, L. Zhang, Z. Zhang, S. Yi and D. Chen, *Appl. Catal. B Environ*., 2022, **317**, 121729.

9 T. Singh, G. Rajeshkhanna, U. Pan, T. Kshetri, H. Lin, N. Kim and J. Lee, *Small*, 2021, **17**, 2101312.

10 Y. Yang, Y. Xie, Z. Yu, S. Guo, M. Yuan, H. Yao, Z. Liang, Y. Lu, T. Chan, C. Li, H. Dong and S. Ma, *Chem. Eng. J*., 2021, **419**, 129512.

11 J. Cen, P. Shen and Y. Zeng, *J. Colloid Interface Sci*., 2022, **610**, 213-220.

12 D. Chen, Z. Pu, R. Lu, P. Ji, P. Wang, J. Zhu, C. Lin, H. Li, X. Zhou and Z. Hu et al, *Adv. Energy Mater*., 2020, **10,** 2000814.

13 I. Kwon, T. Debela, I. Kwak, Y. Park, J. Seo, J. Shim, S. Yoo, J. Kim, J. Park and H. Kang, *Small*, 2020, **16**, 2000081.

14 Y. Zhang, J. Fu, H. Zhao, R. Jiang, F. Tian, R. Zhang, *Appl. Catal. B Environ*., 2019, **257**, 117899.

15 D. Wang, Q. Li, C. Han, Q. Lu, Z. Xing, X. Yang, *Nat. Commun*., 2019, **10**, 3899.

16 J. Liu, Y. Zheng, Y. Jiao, Z. Wang, Z. Lu, A. Vasileff, S. Qiao, *Small*, 2018, **14**, 1704073.

17 H. Zhang, X. Li, A. Hähne, V. Naumann, C. Lin, S. Azimi, S. Schweizer, A. Maijenburg, R. Wehrspohn, *Adv. Funct. Mater*., 2018. **28**, 1706847.